Brain Atlas-based Study of the Interplay between Normal Tissue Microstructural MRI Parameters

I. S. Walimuni[1], and K. M. Hasan[1]
[1]Radiology, UTHSCH, Houston, Texas, United States

Introduction: Magnetic resonance imaging (MRI) provides sensitive microstructural tissue intrinsic metrics such as relaxation, diffusivity and anisotropy that have been used as surrogates of development, aging, therapy and early diagnosis of neurodegenerative disease such as multiple sclerosis [1,2]. MRI parameters such as diffusivity and relaxation are affected by factors that determine the mobility of water molecules such as cellular membranes and myelination. A comprehensive investigation of the interplay between such parameters using standardized volume-based methods in both healthy gray and white matter has not been attempted before. Advances in multimodal MRI registration and segmentation methods have enabled the fusion of high resolution T1, diffusion tensor imaging and relaxation maps to a common native space provided by a high resolution T1-weighted volume. This volume can be anatomically labeled using atlases of white and gray matter regions [3]. In this work, we investigated the interplay between T2 relaxation and the radial diffusivity using 82 brain white matter (WM), gray matter (GM), cortical and subcortical structures. We report, a strong relation between the T2 relaxation and the radial diffusivity in a healthy population.

Methods: *Subjects*: Our cohort included 82 right-handed healthy adult controls with age-matched 41 Men and 41 Women (age range 18-60 years). *Conventional and DT- MRI Acquisition*: MRI studies were performed on a 3T Philips Intera scanner with a dual quasar gradient system and an eight channel SENSE-compatible head coil. The MRI protocol that included a T1-weighted 3D-SPGR volume with isotropic voxel size of 0.9375 mm, dual fast spin-echo sequence with TE_1, TE2 and TR of 11, 90 and 6800 msec respectively. The DTI data were acquired using a single-shot spin-echo diffusion sensitized EPI sequence with the balanced *Icosa21* encoding scheme [2,4] with acquisition parameters, b, T_R, T_E, slice thickness, number of axial slices and field of view (FOV) of 1000 sec mm^{-2}, 6100 msec and 84 msec, 3 mm, 44 and 24 cm respectively. *Data Processing*: Cortical and subcortical tissue segmentations were obtained by the application of FreeSurfer software on the T1-weighted volume [5,6]. These segmentations were used to generate an atlas from each T1-weighted volume in its native space using a method described previously [7]. The T2 transverse relaxation time (T2) and proton density (PD) maps were obtained from the dual echo sequence [2]. The DTI analysis pipeline provided fractional anisotropy (FA), mean diffusivity (D_{av}), axial and radial diffusivity ($\lambda_\perp$) [4]. As shown pictorially in **Figure 1**, T2-weighted and FA images were registered along with their family members (b0, FA, D_{av}, $\lambda_\perp$) to T1-wighted space according to the processing pipeline described elsewhere [7]. As shown in **Figure 3**, segmentations obtained using the brain atlas were further grouped without laterality into, gray matter and white matter regions of frontal, temporal, parietal, occipital, cingulate and deep gray matter [8]. The regional tissue averages of T2, PD, FA, D_{av} and $\lambda_\perp$ were obtained on each subject. Correlations between those metrics were computed using the Pearson correlation. Here we only report the scatter and correlation between age-averaged T2 relaxation and radial diffusivity.

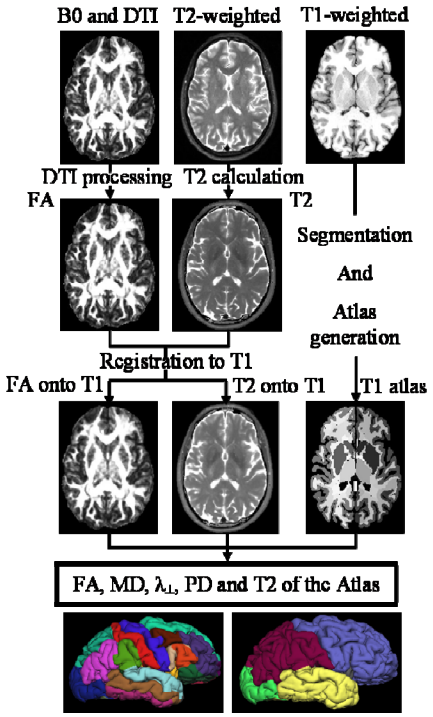

Figure 1: Data processing Pipeline.

Results: **Figure** 2 shows a scatter of the regional mean values of all structures included. Note the heterogeneity and relative values (e.g T2 frontal > parietal > temporal > occipital > cingulate > insula > deep gray matter). Note the strong correspondence between T2 relaxation and the radial diffusivity. Further, a clustering effect is also seen among the structures of the same group. For example, frontal gray matter structures tend to cluster at the top of the distribution (e.g. largest T2 and diffusivity). However, A wide spread distribution can be seen for the deep GM structures. A clear margin of separation is also evident between GM and WM. Strong correlation, heterogeneity and anisotropy of the distribution and the clustering tendency suggest that there is a strong influence with varying degree of strength caused by various brain tissue microstructural attributes upon MRI quantities such as T2 relaxation and radial diffusivity.

Discussion: Due to relatively low water content, higher directionality, and larger myelin content, WM is expected to have a lower T2 and lower $\lambda_\perp$ values compared with gray matter [9]. In GM, water content, cellular membranes and iron content contribute to decrease T2 as shown for the putamen, caudate and globus. A shorter relaxation time value is expected due to its higher iron deposition content which would decrease the T2 [10]. The utility of our two-dimensional quantitative space in modeling the contributors to relaxation (e.g. myelination, water content, iron content) and the application to characterize developing [11] and aging and abnormal tissue is underway.

Referances: [1] Tru C. et al. J Neurol Neurosurg Psychiatry. 2010 (in press). [2] Hasan KM et al., J Magn Reson Imaging. 2009; 29: 70-7 [3] Cherubini, A et al., Neuroimage. 2009;48:29-36. [4] Hasan, KM, Magnetic Resonance Imaging. 2007; 25: 1196–1202. [5] Fischl B et al. Neuron. 2002;33:341-55. [6] Fischl, B et al., Cereb. Cortex. 2004;14:11-22. [7] Walimuni IS et al. Comp. Biol. Med. 2011 (in press). [8] Desikan, RS et al. NeuroImage 2006; 31: 968–80. [9] Cherubini, A et al.,Magnetic Resonance in Medicine. 2009; 61: 1066-1072. [10] Hallgren, B and Sourander, P. Brain J. Neurochem 1958; 3: 41-51. [11] Baratti rt al, Radiology 1999; 210:133-142.

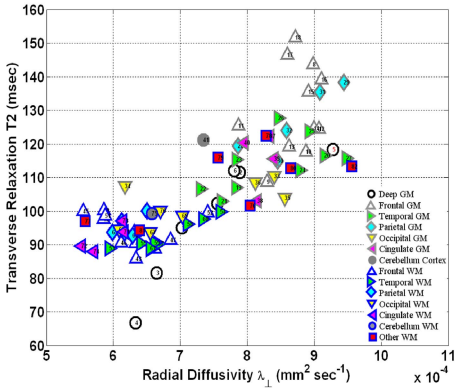

Figure 2: T2 relaxation vs Radial diffusivity. Structures are poc right and left together from FreeSurfer labels and averaged ove ages.

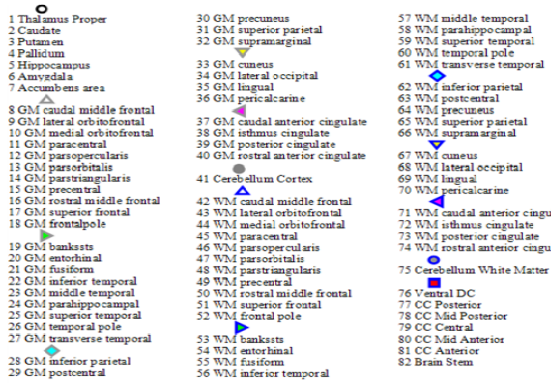

Figure 3: Grouped segmentation labels relevant to **Figure 2**. The symbol at the top the number in front represents each label.